Numerical solution of large $s=\frac{1}{2}$ and $s=1$ Heisenberg antiferromagnetic spin chains using a truncated basis expansion

Mitchel D. Kovarik*
Department of Physics, York University, Toronto, Ontario, Canada M3J 1P3
(Received 28 April 1989; revised manuscript received 11 September 1989)

A new method of determining the spectra of simple quantum-mechanical spin Hamiltonians by direct Hamiltonian-matrix diagonalization is presented. The method is illustrated by applying it to the isotropic one-dimensional Heisenberg antiferromagnet, for which calculations were performed for longer spin chains than by previous direct Hamiltonian-matrix diagonalizations. For spin $s=\frac{1}{2}$ it was possible to accurately determine the ground- and first-excited-state energies for chains of length $N=32$ and 64. For $s=1$ the longest chain for which a similar computation was performed was $N=32$; the singlet-triplet Haldane gap is found to be 0.421 ± 0.005 which is consistent with earlier Monte Carlo results. Long-spin-chain calculations are performed iteratively by solving smaller-chain problems, and constructing from their eigenvalues, and eigenstates, the longer-spin-chain basis and Hamiltonian matrices. The computations were performed on a small computer, which suggests that much larger problems could be handled with a parallel-processing supercomputer.

I. INTRODUCTION

Recently there has been renewed interest in simple one-dimensional (1D) quantum-mechanical models of interacting spins. In spite of the apparent simplicity of these models, there is little understanding of their physical features, and what is known has been obtained through very complex mathematical analysis, or via numerical computations using small clusters of spins. Two recent articles by Müller[1] and Affleck[2] provide an excellent summary of current work.

This revival of interest is due to Haldane's conjecture[3] that the one-dimensional isotropic Heisenberg model has a singlet-triplet energy gap for integral but not half-integral spin. There are a variety of calculations,[4] and some experimental evidence,[5] both supporting and conflicting with this conjecture. However, only the gapless $s=\frac{1}{2}$ case has been solved exactly by Bethe[6] in 1931. Except for $s=\frac{1}{2}$, and 1 it has not been possible to determine the energy gap on a sufficiently long spin chain to determine the infinite-chain limit.

Another interesting problem is the study of the anisotropic $s=\frac{1}{2}$ or 1 antiferromagnetic Heisenberg-Ising ring,[7,8] the XXZ model, with Hamiltonian

$$H=2\sum_{k=1}^{N}[J_x(S_x^kS_x^{k+1}+S_y^kS_y^{k+1})+J_zS_z^kS_z^{k+1}] \quad (1)$$

with $J_z>0$, and where $\mathbf{S}^k=(S_x^k,S_y^k,S_z^k)$ is the spin operator on site k and N is the number of spins in the chain. One introduces an anisotropy parameter Δ by setting $J_x=1-\Delta$ and $J_z=\Delta$. This includes three important cases: (1) the XY case when $\Delta=0$, (2) the Heisenberg case when $\Delta=0.5$, and (3) the Ising case when $\Delta=1$. In the XY phase with $\Delta\ll1$ the ground state is nondegenerate with no long-range magnetic order and a gapless excitation spectrum. In the Néel phase, with $\Delta\approx1$, the ground state is a well-defined doublet with long-range antiferromagnetic order and a spectrum with a nonzero gap. There is a critical Δ in which the system undergoes a localization transition.

Betsuyaku[7-9] and Betsuyaku and Yokota[10] have studied the anisotropic Heisenberg-Ising ring for both $s=\frac{1}{2}$ and 1 by using the results for finite lattices, and then extrapolating to the infinite-N limit. For $s=\frac{1}{2}$ they recover Bethe's analytical result for E_0/N in the infinite-chain limit to six significant figures.

Finite-chain results may be obtained in a variety of ways. Exact ground-state and excited-state energies have been obtained by direct diagonalization of the Hamiltonian matrix via the Lanczos method[11] for up to $s=3$, and by the projector method[7-10] for $s=\frac{1}{2}$ and 1. For the Lanczos and projector methods the memory requirements increase as $(2s+1)^N$ which restricts these calculations to relatively small N ($N=24$ for $s=\frac{1}{2}$, $N=16$ for $s=1$, $N=12$ for $s=\frac{3}{2}$, $N=8$ for $s=2$, $N=6$ for $s=\frac{5}{2}$, and $N=4$ for $s=3$).

For longer spin chains Monte Carlo methods have been employed. Barnes and Daniell[12] used a random-walk algorithm to calculate the ground-state energy and energy gap for $s=\frac{1}{2}$ for spin chains of length up to $N=48$. A Green-function Monte Carlo method[13] has been used to study the structure factor

$$S_N=\sum_{l=1}^{N}\tfrac{4}{3}|\langle\mathbf{S}^k\cdot\mathbf{S}^{k+l}\rangle| \quad (2)$$

in chains of length up to $N=110$ for $s=\frac{1}{2}$. A similar Green-function Monte Carlo method[14] has also been used to study chains of length up to $N=32$ for $s=1$. A new Monte Carlo algorithm based on the Sutherland mapping

has also been used to study long-range correlations for $s=\frac{1}{2}$.[15]

Also, real-space renormalization-group methods have also been used to study quantum-mechanical spin systems in both one and two dimensions. Mattis and Pan,[16] Lin and Pan,[17] and Pan and Chen[18] have studied the infinite-chain limit of the 1D Heisenberg model. In Ref. 16 the Bethe result for the $s=\frac{1}{2}$ ground-state energy per spin was obtained to three significant digits, while in Ref. 17 the $s=1$ ground-state energy density and energy gap obtained were consistent with the previous Monte Carlo calculations of Nightengale and Blöte.[14] In Ref. 18 higher values of s were investigated. In addition, the XY model has been studied for $s=\frac{1}{2}$ and 1.[19] Some earlier renormalization-group results for the 1D Heisenberg model with nearest- and next-nearest-neighbor interactions are presented in Ref. 20.

The recent discovery of high-T_c superconductors[21] and the possibility that their behavior may be described by the magnetic properties of two-dimensional doped antiferromagnets[22] has stimulated considerable interest in the anisotropic two-dimensional Heisenberg model. Monte Carlo methods have been recently applied to the two-dimensional $s=\frac{1}{2}$ problem.[23–27] References 24 and 26 cite various earlier two-dimensional results, including variational, perturbative, spin-wave, mean-field-theory, and direct-diagonalization calculations. Other recent results include a variational calculation of the ground-state wave function[28] and an exact diagonalization of a frustrated Heisenberg model on a 4×4 lattice.[29] Also, the 2D Heisenberg model has recently been studied using the renormalization-group method.[30]

Finite-lattice results may be extrapolated to the infinite-lattice limit, using, for example, the sequence-transformation method of Vanden Broeck and Schwartz.[9,31] It is necessary to determine the energy gap for sufficiently long spin chains to accurately extrapolate to the infinite-chain limit. For $s>1$ exact Hamiltonian-diagonalization methods cannot be applied to sufficiently large lattices, and Monte Carlo methods must be used. As Monte Carlo methods, of course, have various sources of statistical and systematic errors, it would be very useful to assess the accuracy of the Monte Carlo results by comparing to the exact values on very long spin chains for large s. For this reason we have applied a Hamiltonian-matrix-diagonalization method to the determination of energies on long spin chains; this method has been previously applied to scalar-quantum-field theory on a spatial lattice in $1+1$ dimensions.[32]

This paper is organized as follows. Section II contains a brief introduction to the Heisenberg antiferromagnet. In Sec. III the Hamiltonian-matrix-diagonalization method is described. Section IV presents numerical results for $s=\frac{1}{2}$ and 1 and compares these results to previous calculations. Finally, Sec. V contains conclusions and suggestions for future work.

II. THE HEISENBERG ANTIFERROMAGNET

The Hamiltonian for a one-dimensional isotropic Heisenberg model with N spins is

$$H=J\sum_{k=1}^{N}\mathbf{S}^k\cdot\mathbf{S}^{k+1} \tag{3}$$

$$=J\sum_{k=1}^{N}[\tfrac{1}{2}(S_+^kS_-^{k+1}+S_-^kS_+^{k+1})+S_z^kS_z^{k+1}]\ , \tag{4}$$

where $\mathbf{S}^k=(S_x^k,S_y^k,S_z^k)$ is the quantum-mechanical spin operator at site k with $S_\pm^k=S_x^k\pm iS_y^k$. We impose a periodic boundary condition through the identification $\mathbf{S}^{N+1}\equiv\mathbf{S}^1$. In this paper, J is taken to be unity.

A frequently chosen basis for this problem is

$$|m_s^1,m_s^2,\ldots,m_s^N\rangle=|m_s^1\rangle|m_s^2\rangle\ldots|m_s^N\rangle\ , \tag{5}$$

where

$$S_z^k|m_s^i\rangle=m_s^i\delta_{ik}|m_s^i\rangle \tag{6}$$

and

$$S_\pm^k|m_s^i\rangle=[s(s+1)-m_s^i(m_s^i\pm1)]^{1/2}\delta_{ik}|m_s^i\pm1\rangle\ , \tag{7}$$

where s is the total spin, and m_s^i is the z component of the spin at site i.

For $s=\frac{1}{2}$, the ground-state energy per spin and energy gap in the infinite-chain limit have been obtained by Bethe[6] to be

$$\frac{E_0}{N}=\tfrac{1}{4}-\ln2=-0.4431\ , \tag{8}$$

and $E_1-E_0=0$. No similar exact solution for (3) has been obtained for higher s. At each site i there are $2s+1$ values of m_s^i. Thus, the complete basis for a chain of N spins would have $(2s+1)^N$ elements. Since the basis size increases exponentially, this basis is impractical for Lanczos computations for large N. The procedure followed in this work is to truncate the basis space of the system; implementation of this approach is described in the following section.

III. METHOD

The method described below has been previously applied to scalar-quantum-field theory in $1+1$ dimensions.[32] In the quantum-field-theory application, continuous space is replaced by a lattice of points, and the Hamiltonian matrix is written in a basis which is constructed from products of functions at each spatial site. These one-site functions are chosen from one-site Hamiltonian eigenstates, either harmonic or anharmonic eigenfunctions in the scalar field. In principle, this method should be applicable to larger spin systems than quantum-field-theory lattices. This is because the quantum field at each spatial site is continuous and can take on values from $-\infty$ to $+\infty$ whereas each spin can reach only $2s+1$ levels.

Our approach involves the construction of basis states for a spin chain with $N'=aN$ spins ($a=2,3,\ldots$) from a direct product of the eigenstates of a smaller chain ($N=2,3,\ldots$). The Hamiltonian H of the large chain with aN spins may be written as a sum of a N-point spin-chain Hamiltonians plus coupling terms

$$H=H_1+H_{12}+H_2+H_{23}+\cdots+H_a+H_{a1}\ , \tag{9}$$

where H_j is the Hamiltonian of chain j and $H_{j,j+1}$ is the coupling of the final spin of chain j and the initial spin of chain $j+1$. The basis for the long spin chain is chosen to be the product

$$|n_1,\ldots,n_a\rangle=|n_1\rangle\ldots|n_a\rangle\ , \tag{10}$$

where the $|n_i\rangle$'s are eigenstates of the N-spin chain. Here,

$$H_{j,j+1}=\mathbf{S}^k\cdot\mathbf{S}^{k+1}\ , \tag{11}$$

where k denotes the last spin of chain j, and $k+1$ denotes the first spin of chain $j+1$.

This process may be iterated so that chains of $N''=bN'$ spins may be constructed using the energy eigenstates of the N' chain, although it becomes increasingly difficult to determine the N'-chain basis states for a specified accuracy in the final energy.

In the calculations for the subchains of length N we use free boundary conditions, with a coupling of two adjacent chains through $H_{j,j+1}$ terms in the Hamiltonian. If the N' chain is a subchain of a longer chain, the wraparound is not restored. If the N' chain is not a subchain of a still longer chain, the wraparound is restored in that step of the calculation.

For the results presented here the initial subchain had four spins and longer spin chains were constructed by doubling. The 4-spin chain was solved using the basis (5). To reach $N=32$ we iterated the procedure using chains of length 4, 8, and 16. At each stage of the calculation one determines the N_b *lowest* eigenvalues and eigenstates and then computes the matrix elements of S_z, S_+, and S_- at the two endpoints of the chain using these states. This information is used in the next iteration.

The number of states used at each stage should, in principle, be as large as possible to minimize the error in the final result. We find that, in practice, N_b may be chosen to be very much less than the total number of subchain eigenstates. For instance, for a 32-spin chain we chose $N_b=300$ 16-spin eigenstates while the total number of such states is $(2s+1)^{16}$. This fortuitous circumstance is a result of the lowest eigenstates of the 32-spin chain being strongly dominated by the states formed from the lowest eigenstates of the 16-spin subchain. In fact, the lowest 32-spin eigenstates are so strongly dominated by the *lowest* product state, the state giving the lowest diagonal element in the Hamiltonian matrix, that a good estimate of systematic bias may be obtained from understanding this effect. This is described in detail in Sec. IV.

For both $s=\frac{1}{2}$ and 1 the complete set of eigenstates from the 4-spin chain [$(2s+1)^N$ states] was retained for the 8-spin calculation. The lowest 100 states of the 8-spin calculation were then retained for the 16-spin calculation.

The 16-spin-chain basis constructed from the 100 eigenstates of the 8-spin chain has 100^2 elements. We then introduce a truncation procedure to reduce the size of the basis. We define

$$M_n'=\left\langle n\left|\sum_{i=1}^{N'}S_z^i\right|n\right\rangle \tag{12}$$

for some state n of the new basis. The quantity M_n' may be written

$$M_n'=M_k+M_j\ , \tag{13}$$

where $|n\rangle=|k\rangle|j\rangle$ and $|k\rangle$ and $|j\rangle$ are two 8-spin-chain eigenstates. Our truncation involves keeping only those 8-spin-chain eigenstates with $|M_k|$ less than some cutoff, which is then increased to study the resulting bias in the final energies. In these calculations, we decided to keep only those states with $|M_k|\leq 2$. With this truncation it was possible to reproduce previously published results to within a very small error.

One may accelerate the computation by employing the fact that Hamiltonian matrix only has nonzero entries corresponding to states with the same $|M'|$. Thus, ordering the basis according to $|M'|$ gives a block diagonal Hamiltonian matrix. Each block may then be diagonalized separately. For example, in the $s=\frac{1}{2}$ case, keeping only $|M'|=0$ (total $S_z=0$) states this would reduce the complete $(2s+1)^{N'}$ dimensional basis to one with only $[N'!/(N'/2)!(N'/2)!]$ states.

Also, given that the S_+ and S_- are raising and lowering operators, respectively, and that S_z leaves the z component of the spin unchanged, the values of $|M|$ of the states from which the new basis is constructed can be quickly used to determine which of the matrix elements are zero. Suppose a basis state of a $N'=2N$ spin chain is given by $|ab\rangle_{12}=|a\rangle_1|b\rangle_2$, where $|a\rangle_1$ and $|b\rangle_2$ are two eigenstates of the N-spin chain. Then the matrix element ${}_{12}\langle a_m b_m|H_{12}|a_n b_n\rangle_{12}$ is *always* zero unless (1) $M_{a_1}-M_{a_2}=+1$ and $M_{b_1}-M_{b_2}=-1$ or (2) $M_{a_1}-M_{a_2}=-1$ and $M_{b_1}-M_{b_2}=+1$ or (3) $M_{a_1}=M_{a_2}$ and $M_{b_1}=M_{b_2}$.

Most of the computations reported here were carried out on a VAX 6230 computer with three processors, each of which was equivalent to approximately 3 micro VAX's.

The method of matrix diagonalization used is the method of residual minimization and direct inversion in the iterative subspace (RMM-DIIS) of Wood and Zunger.[33] The RMM/DIIS method is particulary well suited to large nonsparse matrices. A major advantage of this method is that the CPU time required scales as the square of the matrix dimension rather than as the cube, assuming that one is interested in computing only the lowest few eigenstates. If the computer program recalculates the matrix elements as needed rather than storing them in computer memory, it is possible to diagonalize very large matrices using this method. For example, to determine the lowest two eigenvalues of a $20\,000\times 20\,000$ matrix (with $N_b\sim 300$) in the last step of a 32-spin calculation (for either $s=\frac{1}{2}$ or 1) required 1.5 VAX-6230 CPU d (using one of the three processors).

The largest memory requirement, approximately 40 megabytes, occurred in the 16- and 32-spin-subchain iterations for $s=\frac{1}{2}$, and for the 16-spin subchain for $s=1$. The total time required for one of these subchain iterations was approximately 10–15 VAX-6230 CPU d, depending on the total load of the machine and whether N was 16 or 32. The 32-spin-subchain calculation took

slightly longer than the 16-spin calculation because the eigenvalues are more closely spaced, and the eigenvectors have, in general, a larger number of significant components. The determination of the eigenvalues took approximately 40% of the time, with the rest spent in the computation of the matrix elements of S_+, S_-, and S_z in the eigenstates. The computations were performed to only seven-figure accuracy to reduce the CPU-time requirements.

IV. RESULTS

A. $s=\frac{1}{2}$

First we wish to estimate the systematic error arising from the basis truncation $|M|\leq k$, where $k=0,1,2,\ldots$. In Table I we present results for the $s=\frac{1}{2}$ 16-spin chain using 8-spin-chain eigenstates with $k=0$, 1, 2, and 4. The exact result is given by the case $|M|\leq 4$. For comparison, we also show the random-walk and Lanczos values of Barnes and Daniell.[12] There is close agreement between the exact result and that obtained using the truncation $|M|\leq 2$. It is clear that the effect of this truncation is generally larger for longer chains, since with each doubling of the chain length additional information is lost.

In Fig. 1 we plot E_0 versus $1/N_b$ for the 16-spin chain. The graph shows a very smooth and very rapid approach to the exact result. This smooth behavior is typical only of problems where one uses a basis which contains a very large proportion of the complete basis. In this case the complete basis with total $S_z=0$ has 12 870 states constructed from $N_b=256$ 8-spin eigenstates. Generally, for longer chains, one is forced to extrapolate to the $N_b=\infty$ limit using some fitting function, chosen to be a linear form for the longer spin chains.

In general, the energy eigenvalues obtained by this method of diagonalization in a truncated Hilbert space give upper bounds to the true values of the energy, the larger the N_b the better the upper bound. The flatness of Fig. 1 indicates that E_0 has converged to within a very small error of the true value for a basis much smaller than the complete one. Thus, in general, a linear fit may not be a good extrapolation technique. However, we find that, for spin chains with $N_b>16$, for which the largest

TABLE I. E_0 and E_1 for various values of $|M|$ for $N=16$ and $s=\frac{1}{2}$. Also shown are exact ($|M|=4$), random walk (RW), and Lanczos (L) results. Here, M is the sum of the z components of the spins of the 8-spin-chain eigenstates.

$\|M\|$	E_0	E_1
0	−6.833 446 34	−6.582 840 16
1	−7.140 156 40	−6.871 134 80
2	−7.142 296 07	−6.872 106 30
Exact	−7.142 296 11	−6.872 106 51
L	−7.1424	−6.8722
RW	−7.138±0.003	−6.864±0.004

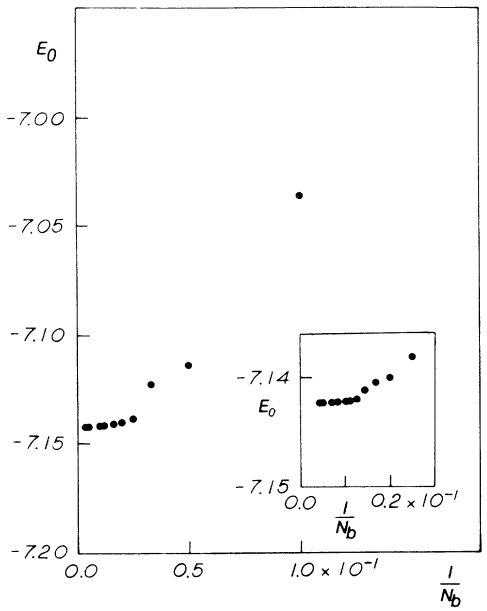

FIG. 1. E_0 vs $1/N_b$ for $N=16$ and $s=\frac{1}{2}$. The largest attainable value for N_b is $N_b=256$ with $1/N_b\approx 0.004$.

value of N_b used is considerably smaller than that required to give the flattening behavior of Fig. 1, the numerical results for the energy eigenvalues are approximately linear in $1/N_b$. In these cases, the energy eigenvalues and energy differences show a substantial change as N_b is increased, even for large N_b. The linear fit may be seen to be a guide to the behavior of the eigenvalues, and gaps as N_b is increased. The "best" upper bound for a eigenvalue obtained using the largest N_b may be a long way from the true value in these cases, and the fitted intercept may give a better value for the eigenvalue (although not necessarily an upper bound). Thus, in accordance with this observed behavior we chose to fit the longer-spin-chain results with a linear form. If the flat region of the graph occurs for N_b much larger than the maximum N_b used (i.e., in the region where $1/N_b$ is very small), the intercept may provide a good approximation to the true value of the energy eigenvalue.

In Figs. 2(a) and 2(b) we display E_0 and E_1 versus $1/N_b$ for $N=32$ and $s=\frac{1}{2}$. Here N_b is the number of 16-spin eigenstates saved from the previous step of the calculation. In Fig. 3 we show the energy gap $\Delta E=E_1-E_0$ versus $1/N_b$. For comparison, in Figs. 2(a) and 2(b) we also show the random-walk results of Barnes and Daniell[12] (BD). The random-walk result of $\Delta E=0.164\pm0.017$ is off the scale of Fig. 3 (the lower limit of $0.164-0.017=0.147$ is marked with an $\times$). Also plotted are values obtained by extrapolating (E) previous finite-chain results for $N\leq 24$ for E_0 and $N\leq 20$ for E_1 and E_1-E_0 also taken from Ref. 12. The new results for $N=32$ are much closer to the extrapolated results than to the results obtained from the random walk. The first thing that one notices upon examination of these graphs is that in Fig. 3 ΔE has converged to approximately 0.1405 ± 0.0005 when $N_b\approx 160$, at which point the values

of E_0 and E_1 are still far from the extrapolated values. When N_b has reached the maximum value of 300 the values of E_0 and E_1 are approximately 0.003 above the extrapolated values, while ΔE still shows signs of fluctuating around the above quoted value. To estimate the $N_b \rightarrow$ complete basis limit, the graphs were fitted with

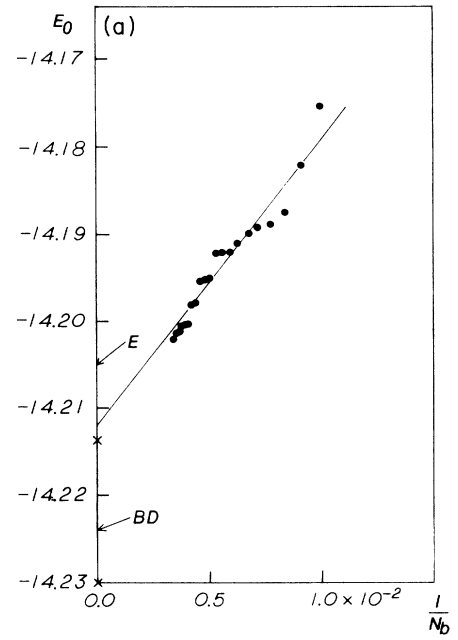

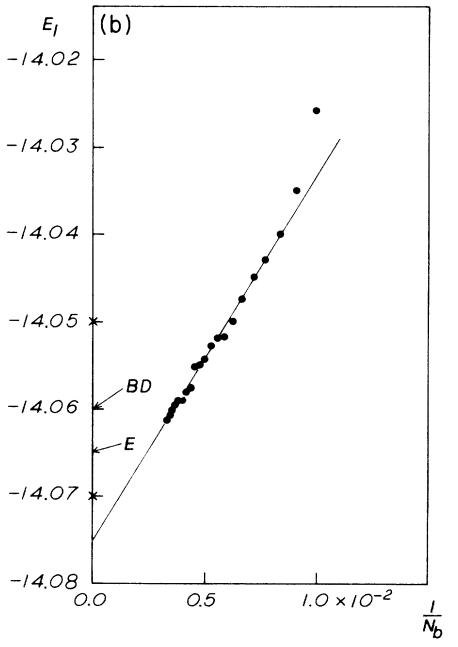

FIG. 2. (a) E_0 vs $1/N_b$ for $N=32$ and $s=\frac{1}{2}$. Also shown is the random-walk result of Barnes and Daniell (BD), and an extrapolation using smaller lattice results (E). The $\times$'s indicate the bounds of the error in the random-walk result. (b) E_1 vs $1/N_b$ for $N=32$ and $s=\frac{1}{2}$. Also shown is the random-walk result of Barnes and Daniell (BD), and an extrapolation of smaller lattice results (E). The $\times$'s indicate the bounds of the error in the random-walk result.

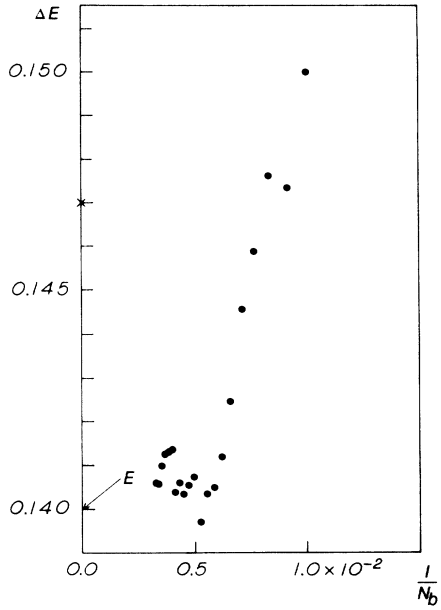

FIG. 3. $\Delta E=E_1-E_0$ vs $1/N_b$ for $N=32$ and $s=\frac{1}{2}$. Also shown is an extrapolation of smaller lattice results (E). The result of Barnes and Daniell is off the scale of the figure. The $\times$ indicates the lower bound of the error in the random-walk result.

straight lines and the intercepts determined. Fitting Figs. 2(a) and 2(b) with straight lines yields intercepts for E_0 and E_1 of -14.212 ± 0.003 (giving $E_0/N=-0.4440$ compared to the extrapolated value of -0.4439) and -14.075 ± 0.003, respectively. We note in passing that E_0 [Fig. 2(a)] is much less linear than E_1 [Fig. 2(b)]. In Fig. 2(a) one sees "terraces" in the slope, which may indicate that E_0 is strongly dominated by a few very important basis states. These terraces are much more pronounced at $N=64$. The errors quoted for the intercepts reflect the statistical error in the fit, and do not include the systematic uncertainty associated with the deviation from linearity.

The region in which the behavior is roughly linear in $1/N_b$ occurs for smaller values of N_b. When it is possible to do so, it is preferable to use larger values of N_b to go beyond this region to where the graphs tend to flatten out. In these situations the linear $1/N_b$ fit using small N_b will not give as good a result as can be obtained by going to larger values. In Fig. 1, the graph of E_0 versus $1/N_b$ is flat when $N_b=256$ ($1/N_b\approx0.004$), but a linear fit including points with $N_b<100$ will clearly yield a good result. For $N=32$ the intercepts are substantially lower than the extrapolated values, and yield $\Delta E=0.13$, which is much lower than both the extrapolated value and the ΔE obtained by the Hamiltonian-matrix-diagonalization method. In any case, the linear fit yields an error of no more than 0.01 from the exact value. Figure 3 is consistent with an extrapolated value of $\Delta E\approx0.14$. In Fig. 3 for $N_b>160$ the gap was found to cluster around a value of approximately 0.1405. This suggests that there must be an error associated with the linear approximation made in fitting Figs. 2(a) and 2(b). Neither Figs. 2(a) nor

2(b) show convincing convergence with increasing N_b. The estimated error of the extrapolated values is approximately ± 0.003. Given the proximity of the $N_b = 300$ values of E_0 and E_1 to the extrapolated values, it is possible that a dramatic flattening out of the graphs could occur for only slightly larger N_b, assuming, of course,

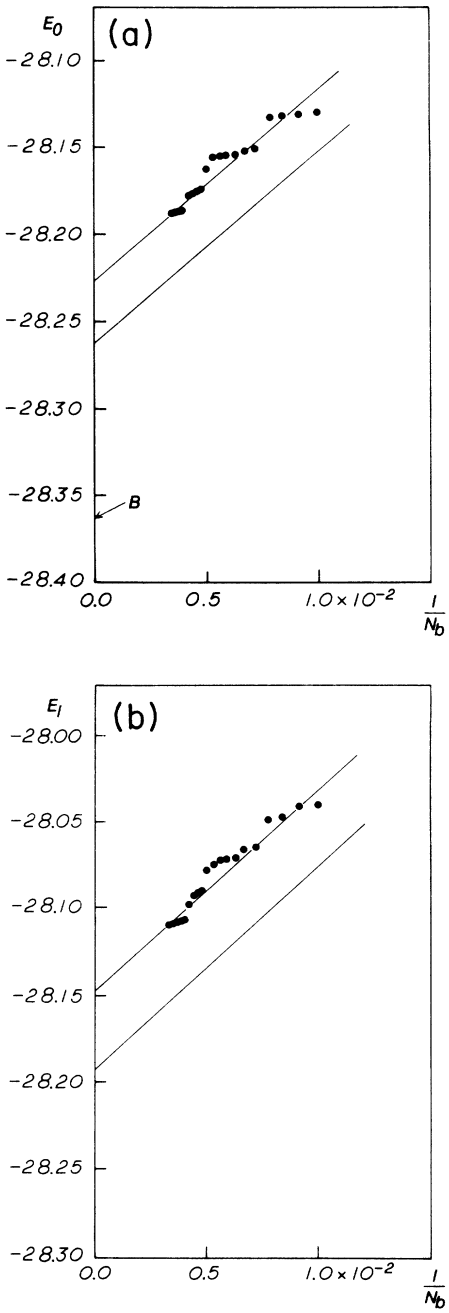

FIG. 4. (a) E_0 vs $1/N_b$ for $n = 64$ and $s = \frac{1}{2}$. The upper line is a result of a linear fit of the data points while the lower is shifted down by the correction $2\delta E_0^{32}$. (B) is the Bethe result for $E_0/N = -0.4431$ in the infinite-N limit. (b) E_1 vs $1/N_b$ for $N = 64$ and $s = \frac{1}{2}$. The upper line is a result of a linear fit of the data points while the lower is shifted down by the correction $\delta E_0^{32} + \delta E_1^{32}$.

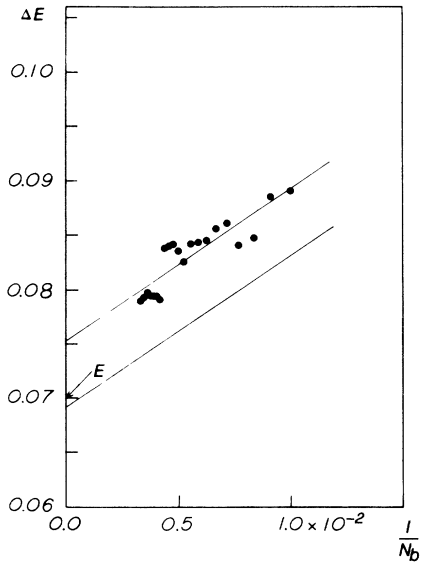

FIG. 5. $\Delta E = E_1 - E_0$ vs $1/N_b$ for $N = 64$ and $s = \frac{1}{2}$. The upper line is a result of a linear fit of the data points while the lower is shifted down by the correction $\delta E_0^{32} + \delta E_1^{32} - 2\delta E_0^{32} = \delta E_1^{32} - \delta E_0^{32}$. ($E$) is the extrapolated value based on smaller chain results.

that the extrapolated values are accurate.

In Figs. 4(a), 4(b), and 5, we show the same information for $N = 64$ and $s = \frac{1}{2}$. Fitting Figs. 4(a) and 4(b) with straight lines yields $E_0 = -28.221 \pm 0.005 (E_0/N = -0.4410)$ and $E_1 = -28.146 \pm 0.005$, with an energy gap of $\Delta E = 0.075 \pm 0.004$. The relatively small error of ΔE is from the fit of Fig. 5. The terracing seen in Fig. 2(a) is considerably more pronounced in Fig. 4(a). This suggests that a simple linear fit of the data points may incorporate an important systematic error. These numbers are far above what one would expect, given the Bethe result $E_0/N = -0.4431$ and $\Delta E = 0$ as $N \to \infty$. Previous results[12] suggest that $\Delta E \approx 0.07$ for $N = 64$. Some of this discrepancy can be easily explained by considering the accuracy of the eigenstates of the 32-spin subchain computation. The results for the 32-spin chain presented in Figs. 2(a), 2(b), and 3 were obtained using linear fits with N_b's up to 300. In the 32-spin-subchain calculation only $N_b = 100$ states were used, giving a substantial error. We shall now give an estimate of the size of this systematic bias.

The ground-state energy can be written

$$E_0 = c_{00}^2 \, {}_{32}\langle 0| \, {}_{32}\langle 0|H|0\rangle_{32} \, |0\rangle_{32} + \sum_{i,j,k,l} c_{ij} c_{kl} \, {}_{32}\langle i| \, {}_{32}\langle j|H|k\rangle_{32} \, |l\rangle_{32} , \qquad (14)$$

where the c_{mn}'s are the components of the normalized eigenvector corresponding to E_0, and where the summation is carried out over all the terms in the series excluding the $ij,kl = 00,00$ term, and where the $|i\rangle_{32}$'s are the N_b eigenstates of the 32-spin subchain with free boundary conditions. In the diagonal approximation this becomes

$$E_0 = c_{00}^2\,{}_{32}\langle 0|\,{}_{32}\langle 0|H|0\rangle_{32}\,|0\rangle_{32} + \sum_{i,j} c_{ij}^2\,{}_{32}\langle i|\,{}_{32}\langle j|H|i\rangle_{32}\,|j\rangle_{32} \,. \quad (15)$$

The diagonal approximation is a reasonable one to make since the off-diagonal Hamiltonian-matrix elements are very small ($\ll 0.1$) and have very small absolute errors, and their contribution to the energy eigenvalue is further reduced by the product of the corresponding coefficients of the eigenvector. The first term of (15) is equal to

$$c_{00}^2(E_0^{32}+E_0^{32}) = 2c_{00}^2 E_0^{32} \,, \quad (16)$$

where E_0 is the lowest energy of the 32-spin subchain. In general,

$$\delta E_i^{32} \geq \delta E_0^{32} \quad \text{for } i>0 \quad (17)$$

since excited states usually converge much more slowly. We also use the further approximation $\delta E_i^{32}=\delta E_0^{32}$ for $i>0$. The systematic correction to E_0 is then approximately $2\times\delta E_0^{32}$. Since the ground state is dominantly $|0\rangle_{32}|0\rangle_{32}$ this is probably a reasonable estimate of this bias. The value of δE_0^{32} is implicit in Fig. 2(a); δE_0^{32} is approximately one-half the difference between E_0 at $N_b=100$ and the fitted intercept, giving $\delta E_0^{32}=0.0183$. The factor of one-half occurs because we are dealing with a subchain without wraparound, so that there are effectively half as many interactions as are present with periodic boundary conditions. The bias in the diagonal element is then approximately $2\times\delta E_0^{32}=0.0366$. Applying this as a correction to the lowest eigenvalue of the 64-spin chain gives $E_0=-28.258\pm0.005$, which leads to $E_0/N=-0.4415$.

Similarly the bias in E_1 is determined from that of the diagonal elements corresponding to states $|0\rangle_{32}|1\rangle_{32}$ and $|1\rangle_{32}|0\rangle_{32}$ (where $|0\rangle_{32}$ and $|1\rangle_{32}$ have $M=0$) which are the dominant components of the first excited state of the 64-spin chain. This correction is given by $\delta E_0^{32}+\delta E_1^{32}$ where δE_1^{32} is taken from Fig. 2(b) as was δE_0^{32}. δE_1^{32} was found to be 0.0245, giving a correction of $0.0183+0.0245=0.0428$ and a corrected value of $E_1=-28.189\pm0.005$.

The corrected value of the energy gap is $\Delta E=0.069\pm0.004$. This is very close to the estimated value of ~ 0.07, and supports our procedure for removing this systematic bias from the energies. The outstanding significant discrepancy between the ground-state energy and Bethe's result suggests, however, that this approximation may not be sufficiently accurate. It is possible that a study of the errors of the excited states of the 32-chain basis could resolve this discrepancy.

We have also tried fitting Figs. 4(a) and 4(b) after discarding the points in the two large terraces between $N_b=100$ and 180. This gave $E_0=-28.258\pm0.005$ and $E_1=-28.187\pm0.005$, respectively, so that we find $\Delta E=0.071\pm0.004$. The corrected values are then $E_0=-28.295\pm0.005$ and $E_1=-28.230\pm0.005$, giving $E_0/N=-0.4421$ and $\Delta E=0.065\pm0.004$. Given the large errors in these numerical fits, it seems that for $N=64$ ΔE cannot be determined to better than approxi-

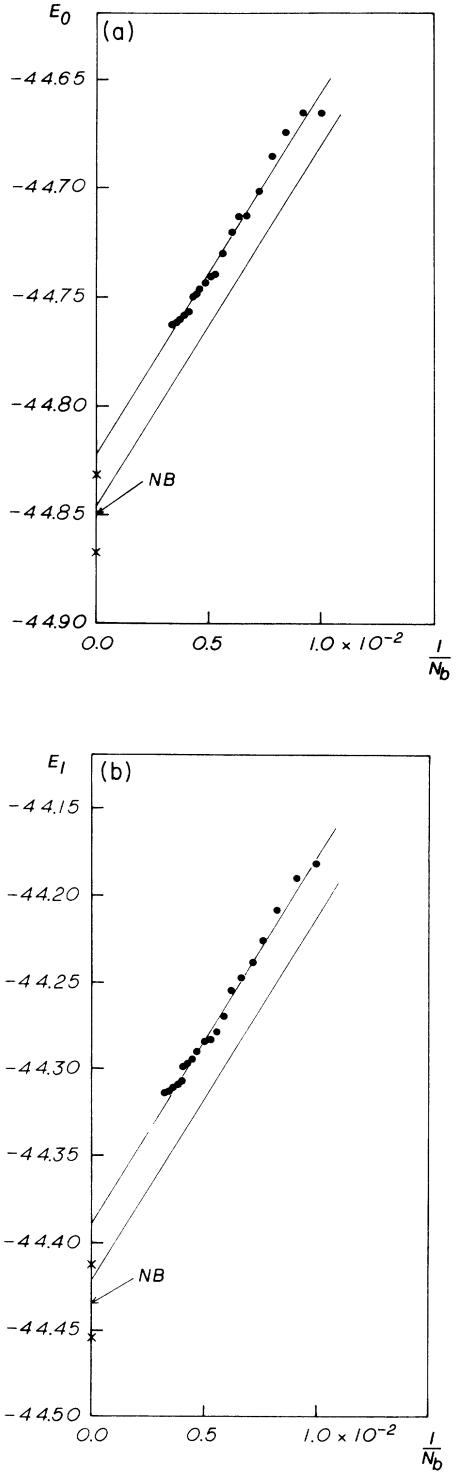

FIG. 6. (a) E_0 vs $1/N_b$ for $N=32$ and $s=1$. The upper line is a result of a linear fit of the data points while the lower is shifted down by the correction $2\delta E_0^{16}$. Also shown is the result of Nightengale and Blöte (NB). The $\times$'s indicate the bounds of the error in the result of Nightengale and Blöte. (b) E_1 vs $1/N_b$ for $N=32$ and $s=1$. The upper line is a result of a linear fit of the data points while the lower is shifted down by the correction $\delta E_0^{16}+\delta E_1^{16}$. Also shown is the result of Nightengale and Blöte (NB). The $\times$'s indicate the bounds of the error in the result of Nightengale and Blöte.

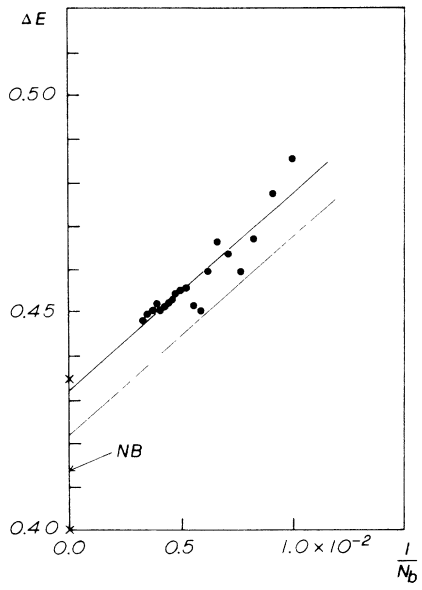

FIG. 7. $\Delta E = E_1 - E_0$ vs $1/N_b$ for $N=32$ and $s=1$. The upper line is a result of a linear fit of the data points while the lower is shifted down by the correction $\delta E_0^{16} + \delta E_1^{16} - 2\delta E_0^{16} = \delta E_1^{16} - \delta E_0^{16}$. Also shown is the result of Nightengale and Blöte (NB). The ×'s indicate the bounds of the error in the result of Nightengale and Blöte.

mately ±0.005 with our present understanding of systematic effects and statistical errors.

B. $s=1$

For $N=16$ and $s=1$ we obtained $E_0 = -22.446 \pm 0.005$ and $E_1 = -22.005 \pm 0.005$ while the results of Nightengale and Blöte[14] are -22.4463 ± 0.005 and -22.0049 ± 0.005. The size of the error quoted with the results of Nightengale and Blöte were estimated from a visual inspection of Fig. 2 of their paper. The $N_b \to \infty$ values were obtained from linear fit of the numerical results versus $1/N_b$ for N_b up to 200.

In Figs. 6(a) and 6(b) we plot E_0 and E_1 versus $1/N_b$ for $N=32$ and $s=1$. In Fig. 7 we plot the energy gap $\Delta E = E_1 - E_0$ versus $1/N_b$. For comparison, we also show the Green-function Monte Carlo results of Nightengale and Blöte.[14] Again, we fitted the data with a linear form; the intercepts determined gave $E_0 = -44.820 \pm 0.005$ and $E_1 = -44.391 \pm 0.005$ while those of Nightengale and Blöte are -44.8497 ± 0.015 and -44.4364 ± 0.015. The two sets of numbers are within acceptable error of each other. The results of the Hamiltonian-matrix diagonalization were consistently higher than those of Nightengale and Blöte. The $N=16$ results quoted above suggest that choosing $|M| \leq 2$ is probably sufficient. However, in the next to last step where the 16-spin lattice was solved, only $N_b = 100$ basis states were used, while the extrapolation for the 16-spin chain with wraparound quoted above was obtained using N_b's up to 200. These results suggest that for $N_b = 100$ the 16-spin-subchain results cannot be well converged. Thus, it was necessary to correct the results following the prescription described above, obtaining $\delta E_0^{16} = 0.0125$ and $\delta E_1^{16} = 0.0195$, giving $E_0 = -44.845 \pm 0.005$ and $E_1 = -44.424 \pm 0.005$. The agreement between the corrected numbers and those of Nightengale and Blöte is remarkable. The Nightengale and Blöte numbers give $\Delta E = 0.4133 \pm 0.02$ while the corrected Hamiltonian-matrix diagionalization gives $\Delta E = 0.421 \pm 0.005$. This

TABLE II. Summary of E_0, E_1, and ΔE at indicated maximum values of N_b, corrected values at the indicated maximum values of N_b (corr.), linear extrapolations (lin. ext.), corrected linear extrapolations (corr. lin. ext.), extrapolations using results with chains with $N < 32$ (ext.), and the random-walk results of Barnes and Daniell (RW) for $s = \frac{1}{2}$. The values for E_0 and E_1 obtained at $N_b = 300$ are the best upper bounds for these eigenvalues for 32 and 64, respectively. The $N=16$ results are exact.

	E_0	E_1	ΔE
	$N=16$		
$N_b=256$	−7.142 296 11	−6.872 106 51	0.270 189 60
	$N=32$		
$N_b=300$	−14.201 975 74	−14.061 392 21	0.140 583 53
Lin. ext.	−14.212±0.003	−14.075±0.003	0.13±0.01[a]
RW	−14.224±0.010	−14.06±0.02	0.164±0.017
Ext. $N<32$	−14.2048	−14.065	0.14
	$N=64$		
$N_b=300$	−28.188 320 05	−28.109 342 76	0.078 977 29
$N_b=300$ corr.	−28.2249	−28.1521	0.0728
Lin. ext.	−28.221±0.005	−28.146±0.005	0.075±0.004
Corr. lin. ext.	−28.258±0.005	−28.189±0.005	0.069±0.004
Ext. $N \leq 32$			0.07[b]

[a] ΔE obtained from $E_1 - E_0$ and not from a fit of Fig. 3.
[b] ΔE extrapolated from finite-chain gaps with $N \leq 32$ and not from the difference of the extrapolations of the corresponding finite-energy eigenvalues.

TABLE III. E_0, E_1, and ΔE at indicated maximum value of N_b, corrected values at the indicated maximum value of N_b (corr.), linear extrapolations (lin. ext.), corrected linear extrapolations (corr. lin. ext.), and the results of Nightengale and Blöte (NB) for $s=1$. The values for E_0 and E_1 obtained at $N_b=300$ are the best upper bounds for these eigenvalues.

	E_0	E_1	ΔE
	$N=16$		
$N_b=195$	−22.440 275 72	−21.991 180 77	0.449 014 95
Lin. ext.	−22.446±0.005	−22.005±0.005	0.441±0.005
NB	−22.4463±0.005	−22.0049±0.005	0.4414±0.007
	$N=32$		
$N_b=300$	−44.761 730 76	−44.313 232 95	0.447 497 81
$N_b=300$ corr.	−44.7867	−44.3452	0.4415
Lin. ext.	−44.820±0.005	−44.391±0.005	0.429±0.005
Corr. lin. ext.	−44.845±0.005	−44.424±0.005	0.421±0.005
NB	−44.8497±0.015	−44.4364±0.015	0.4133±0.02

was obtained in two ways, by fitting Figs. 6(a) and 6(b) with straight lines, and taking the difference of the intercepts, and also by fitting Fig. 7 with a straight line directly, and then applying the correction. The uncorrected energy gap was $\Delta E=0.430\pm0.005$. Figures 6(a) and 6(b) were remarkably linear for the range of N_b studied. Figure 7 showed linear behavior only for large N_b between 240 and 300. This lends credibility to the expectation that were N_b to be increased, no change in the behavior of the graph would occur, and a linear fit should be sufficient.

V. CONCLUSIONS

In this paper we have demonstrated a new method of determining the spectra of the one-dimensional isotropic Heisenberg model. Using a direct-diagonalization algorithm with a truncated basis, calculations were performed for $s=\frac{1}{2}$ and 1 on spin chains which were much longer than those for which computations had previously been done by direct matrix diagonalization. We summarize our numerical results in Tables II and III for $s=\frac{1}{2}$ and 1, respectively. We compare our values for E_0, E_1, and ΔE (best upper bounds, linear extrapolations, and corrected linear extrapolations) with previously published results, where available. We found that our results agreed to within a small error with those obtained by other methods.

The new method is time and computer-memory intensive, but it seems likely that implemenation of this method on fast-parallel or vector machines may allow accurate determinations of quite long-spin-chain energies in future applications.

In particular, it would be very interesting to apply this method to the two-dimensional anisotropic Heisenberg model which is a model for magnetic effects in high-T_c superconductors. Barnes *et al.*[26] have shown that a rectangular 8×8 spin array with 64 spins is sufficiently large for numerical study of various aspects of anisotropic Heisenberg models. Since the longest spin chain studied in this work had 64 spins, it seems plausible that the new method could be easily modified to study the two-dimensional Heisenberg models and related systems with comparable basis-size requirements.

ACKNOWLEDGMENTS

I wish to thank Ted Barnes, John Liakos, and Roser Valenti for many useful conversations. I wish to thank C. Y. Pan for providing a number of references for some recent renormalization-group results. I am grateful to the York Computing Services without whose assistance this work would not have been possible. In addition, I would also like to thank the Department d'Estructura i Constituents de la Matèria of the Facultat de Fisica of the Universitat de Barcelona, and the Theory Group of the Department de Fisica of the Universitat Autonoma de Barcelona where much of the computer programming for this work was done. I wish to thank Roman Koniuk and the Natural Sciences and Engineering Research Council of Canada for providing financial support.

*Present address: Physics Department, University of Tennessee, Knoxville, TN 37996.

[1]G. Müller, Z. Phys. B **68**, 149 (1987).
[2]I. Affleck, J. Phys. **1**, 3047 (1989).
[3]F. D. M. Haldane, Bull. Am. Phys. Soc. **27**, 181 (1982); Phys. Lett. **93A**, 464 (1983); Phys. Rev. Lett. **50**, 1153 (1983).
[4]S. T. Chui and K. B. Ma, Phys. Rev. B **29**, 1287 (1984); J. Sólyom and T. Ziman, *ibid.* **30**, 3980 (1984); J. Sólyom, *ibid.* **32**, 7524 (1985); J. Schulz and T. Ziman, *ibid.* **33**, 6545 (1986); J. Schulz, *ibid.* **34**, 6372 (1986).
[5]W. J. L. Buyers, R. M. Morra, R. L. Armstrong, M. J. Horgan, P. Gerlach, and K. Hirakawa, Phys. Rev. Lett. **56**, 371 (1986); R. M. Morra, W. J. L. Buyers, R. L. Armstrong, and K. Hirakawa, Phys. Rev. B **38**, 543 (1988).
[6]H. Bethe, Z. Phys. **71**, 205 (1931).
[7]H. Betsuyaku, Phys. Rev. B **36**, 5613 (1987).

[8]H. Betsuyaku, Phys. Rev. B **36**, 799 (1987).
[9]H. Betsuyaku, Phys. Rev. B **34**, 8125 (1986).
[10]H. Betsuyaku and T. Yokota, Phys. Rev. B **33**, 6505 (1986).
[11]H. W. J. Blöte, Physica **93B**, 93 (1978); J. C. Bonner and J. B. Parkinson, Phys. Rev. B **32**, 4703 (1985); E. R. Gagliano, E. Dagotto, A. Moreo, and F. C. Alcaraz, *ibid.* **34**, 1677 (1986); A. Moreo, *ibid.* **35**, 8562 (1987).
[12]T. Barnes and G. J. Daniell, Phys. Rev. B **37**, 3637 (1988).
[13]J. R. Borysowicz, A. Moreo, T. A. Kaplan, and K. Kubo, Nucl. Phys. B **300**, 301 (1988).
[14]M. P. Nightengale and H. W. Blöte, Phys. Rev. B **33**, 659 (1986).
[15]K. Kubo, T. A. Kaplan, and J. R. Borysowicz, Phys. Rev. B **38**, 11 550 (1988).
[16]D. C. Mattis and C. Y. Pan, Phys. Rev. Lett. **61**, 463 (1988).
[17]H. Q. Lin and C. Y. Pan, J. Phys. (Paris) **C8**, 1415 (1988).
[18]C. Y. Pan and X. Chen, Phys. Rev. B **36**, 8600 (1987).
[19]C. Y. Pan and H. Q. Lin, J. Appl. Phys. **64**, 5932 (1988).
[20]P. M. Vanden Broek, W. J. Caspers, and M. W. M. Willemse, Physica **104A**, 298 (1980); D. C. Mattis and R. Schilling, J. Phys. C **14**, L729 (1981).
[21]J. G. Bednorz and K. A. Müller, Z. Phys. B **64**, 189 (1986).
[22]P. W. Anderson, Science **235**, 1196 (1987).
[23]J. D. Reger and A. P. Yound, Phys. Rev. B **37**, 5978 (1988); I. Morgenstern and D. Wurtz, Z. Phys. B **70**, 115 (1988); P. Horsch and W. von der Linden, *ibid.* **72**, 181 (1988); E. Manousakis and R. Salvador, Phys. Rev. B **39**, 575 (1989); G. Gomez-Santos, J. D. Joannopoulos, and J. W. Negele, *ibid.* **39**, 4435 (1989).
[24]T. Barnes and E. S. Swanson, Phys. Rev. B **37**, 9405 (1988).
[25]T. Barnes, in *Proceedings of the Computational Atomic and Nuclear Physics at One Gigaflop Conference,* Vol. 16 of *Nuclear Science Research Conference Series,* edited by C. Bottcher, M. R. Strayer, and J. B. McGrory (Harwood Academic, New York, 1989), pp. 83–106.
[26]T. Barnes, D. Kotchan, and E. S. Swanson, Phys. Rev. B **39**, 4357 (1989).
[27]T. Barnes, K. J. Cappon, E. Dagotto, D. Kotchan, and E. S. Swanson, Phys. Rev. B **40**, 8945 (1989).
[28]C. Dasgupta, Phys. Rev. B **39**, 386 (1989).
[29]E. Dagotto and A. Moreo, Phys. Rev. B **39**, 4744 (1989).
[30]C. Y. Pan, Int. J. Mod. Phys. **3**, 1435 (1989); **3**, 1443 (1989).
[31]J. M. Vanden Broeck and L. W. Schwartz, SIAM J. Math. Anal. **10**, 658 (1979); C. J. Hamer and M. N. Barber, J. Phys. A **14**, 2009 (1981); M. N. Barber and C. J. Hamer, J. Aust. Math. Soc. Ser. B **23**, 229 (1982).
[32]M. D. Kovarik, J. W. Darewych, and R. Koniuk, Phys. Rev. D **32**, 2646 (1985); **33**, 3654 (1986); M. D. Kovarik and R. Koniuk, *ibid.* **38**, 2537 (1988).
[33]D. M. Wood and A. Zunger, J. Phys. A **18**, 1343 (1985).